POLITECNICO
MILANO 1863

SCUOLA DI INGEGNERIA INDUSTRIALE
E DELL'INFORMAZIONE

Simulating Aeration at Birth: building an Open-Source Newborn Lung Model

Tesi di Laurea Magistrale in
Biomedical Engineering - Ingegneria Biomedica

Luca Andriotto, 928454

Advisor:
Prof. Raffaele Dellaca'

Co-advisors:
Dr. Chiara Veneroni

Academic year:
2023-2024

Abstract: During pregnancy, the fetal airways are filled with a fluid known as fetal lung fluid, which is essential for the development of airways. Consequently, at birth, the respiratory system must expel this fluid to allow aeration. Preterm infants may not be able to adequately achieve lung aeration at birth autonomously. The application of a positive pressure waveform at the airway opening can support them. However, the best pressure strategy for promoting lung aeration without damaging the fragile lung is still unknown. Model simulation can help in the definition of such a strategy. Aims of this projects are: 1) Generate a model from neonatal CT scans to optimize the generation of airways, ensuring they adhere to the morphometric characteristics at various ages. 2) Develop an open-source mechanical model that allows for the simulation of mechanical properties along with fluid dynamics. Using a CT scan of a newborn infant, we extracted the centreline of major airways and the lobe surfaces. We then reconstructed the anatomy of the missing airways using a statistical algorithm originally proposed for adult lungs, which we adapted for the newborn lung. This algorithm assigned airway diameters based on proportions measured in the newborn lung. We implemented a mechanical analog of the airway and acini in Julia, a free and open source programming language allowing to construct modularly complex ODE systems and to solve them. This model accounts for changes related to aeration at birth, allowing the simulation of the flow of fetal fluid towards the periphery as air enters the airways.

Key-words: morphometric model, aeration process, lung, newborn, respiratory system

1. Introduction

During pregnancy, the fetal airways are filled with a fluid known as fetal lung fluid, which is essential for developing airways. Consequently, at birth, the respiratory system must expel this fluid to allow air to enter and exit, a process necessary for breathing (aeration). Fluid reabsorption begins a few days before birth through chemical processes involving Na^+ channels, and during natural childbirth, fluid is expelled from the mouth and nose due to the compression of the neonate's chest. In full-term infants, the likelihood of complications during aeration is very low. However, the scenario is vastly different for preterm infants, who are born before 37 weeks of gestation compared to the typical 40 weeks of a normal pregnancy.

Applying pressure at the entrance of the airways helps preterm infants remove the fluid and open the closed acini. Once the acini are recruited, less pressure is needed to keep them open and ventilate the lung. Thus, employing recruitment strategies at birth has the advantage of initiating ventilation in a more recruited lung, using lower pressures, achieving more homogeneous lung aeration, and reducing the stress applied to the tissues. It is important to note, however, that at birth, the lung is more delicate and thus more susceptible to damage, even with routine ventilation procedures. Therefore, developing protective recruitment strategies at birth could lead to significant improvements in this area.
Although recruitment maneuvers have gained more interest in preterm ventilation, there is still no common medical strategy. Experimental procedures are tested on animals, presenting challenges in obtaining results due to the invasiveness of the procedures and associated ethical issues[8, 4]. In silico modeling of the adult lung has been useful for understanding pathophysiology and making diagnoses. Thus, the same approach could help analyze various recruitment strategies and their impact on the lung during initial aeration at birth. However, in silico models of neonatal lungs are limited to describing up to the first generation of the bronchial tree resulting inadequate for simulating the physiological changes that occur at birth. Anatomical models of the adult lung were scaled to match the newborn one. However, there are differences between airway length and diameter proportion between infants and adults[6]. Moreover, the immature lung structure results in different mechanical properties[13].
Consequently, both the anatomical and mechanical characteristics of the tissues must be appropriately modified to achieve a consistent model for the neonatal case in the time domain. Finally, to implement the changes occurring at birth, the mechanical properties of each airway must change when the fetal fluid is replaced by air. A previous thesis work developed an in silico model able to simulate the mechanical changes occurring in the airways during aeration at birth in the time domain. However, the anatomical structure was scaled for the adult one, and the mechanical model was implemented in «CADENCE», a platform optimized for the analysis of integrated circuits. The use of «CADENCE» platform results in limitations related to the need for proprietary software licenses and difficulties in implementing time-varying phenomena not easily described by standard electronic components.
Using open-source strategies for the model eliminates the need for proprietary software licenses, making the development process more accessible[12].
The aims of this project are:

Generate a model from neonatal CT scans to optimize the generation of airways, ensuring they adhere to the morphometric characteristics at various ages.

Develop an open-source mechanical model that allows for the simulation of mechanical properties along with fluid dynamics.

2. Preterm Neonates

2.1. Challenges and Characteristics

A baby born before reaching thirty-seven weeks of pregnancy is considered preterm. Typically, a full-term pregnancy lasts about forty weeks. Preterm births can be further classified based on how early the baby is born:

- Extremely preterm: Birth occurs before twenty-eight weeks.
- Very preterm: Birth happens between twenty-eight and thirty-two weeks.
- Moderate to late preterm: Birth occurs between thirty-two and thirty-seven weeks.

This issue should not be underestimated, as fifteen million babies are born preterm each year[16]. Preterm infants often have underdeveloped lungs. Respiratory insufficiency in these babies can be managed with ventilation support.

2.2. Liquid Clearance

The respiratory transition from liquid to air in newborns involves three stages:

1. No pulmonary gas exchange
2. Liquid clearance and initiation of gas exchange
3. Removal of residual liquid

Initially, the baby cannot breathe because the lungs are still filled with liquid. Two main factors influence the absorption of this liquid:

- *Gestational Age*
- *Mode of Delivery* (either vaginal or cesarean section)

Before the baby can start breathing air, the liquid must be cleared from the lungs. A significant contribution to this process comes from a chemical mechanism: Na^+ reabsorption. The stress of labor increases levels of adrenaline and vasopressin, which drive this process. These hormones stimulate the airway epithelium to reverse the osmotic gradient, leading to liquid uptake.
During birth, the liquid is expelled from the lungs through the nose and mouth, a process known as the "vaginal squeeze." This process involves changes in fetal posture, such as increased spinal flexion, which elevates the diaphragm and increases abdominal and transpulmonary pressure.
The pressure gradient is crucial for driving air movements throughout the lungs.
Transpulmonary pressure is the difference between alveolar pressure and pleural pressure in the pleural cavity. If transpulmonary pressure is zero, no air movement occurs. If it is positive or negative, air flows out or in, respectively.
The presence of liquid in the interstitial compartment increases pressure. As the alveolus empties and its pressure decreases, a small amount of liquid re-enters, initiating a continuous cycle of liquid clearance and re-entry in the alveolus.

2.3. Analogies and Differences with Adult Lung

The respiratory system of a neonate presents both similarities and differences compared to that of an adult.
A common aspect is the number of airways. By the end of gestation, the branching of the bronchial tree is complete.
The differences lie in the size of the airways. The peripheral airways in neonates, which are the smallest, are about half the size of those in adults. However, the trachea in neonates is about one-third to one-fourth the size of an adult's trachea, indicating no consistent scaling rule.
The number of alveoli is also different. Infants have fewer alveoli than adults, as their development and proliferation continue until about eight years of age [1].
Beyond anatomical differences, neonates also differ in mechanical properties.
Neonates have higher airway resistance compared to adults, which decreases continuously during the first year of life.
The thorax of neonates is highly compliant and deformable due to the thin cartilage of the ribs and incomplete mineralization of the bones.
Thoracic compliance decreases during the first year of life.
Additionally, neonates' ribs are positioned more horizontally, reducing the efficiency of the respiratory muscles.

3. Anatomical Models

The structure of the internal lung is significantly influenced by the hierarchical arrangement of the airways, which resemble a fractal branching tree[18]. The design of this airway tree is crucial for its function, as the branching pattern affects airflow and particle deposition. In modeling the human airway tree, it is widely accepted that the airways follow an irregular dichotomy pattern. Unlike regular dichotomy, where each branch splits into two identical daughter branches, irregular dichotomy results in daughter branches that can vary significantly in length and diameter.

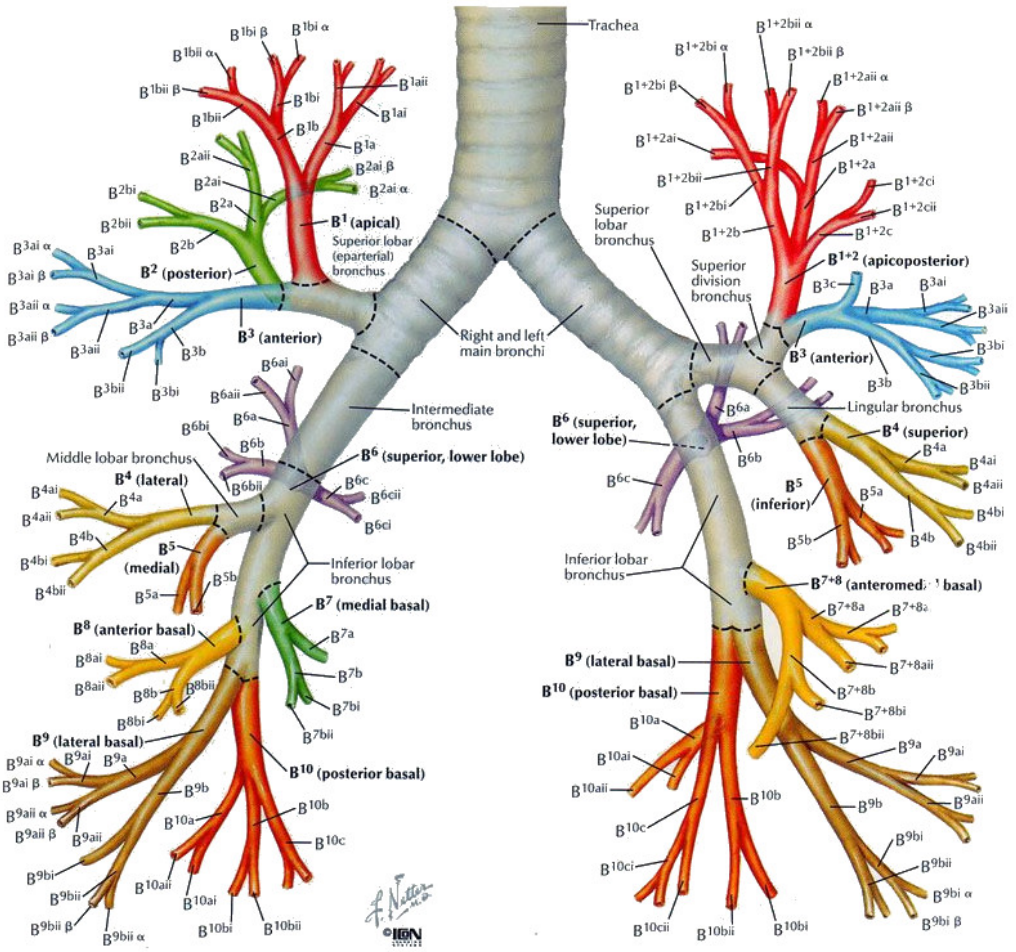

Figure 1: Representation of the major airways.

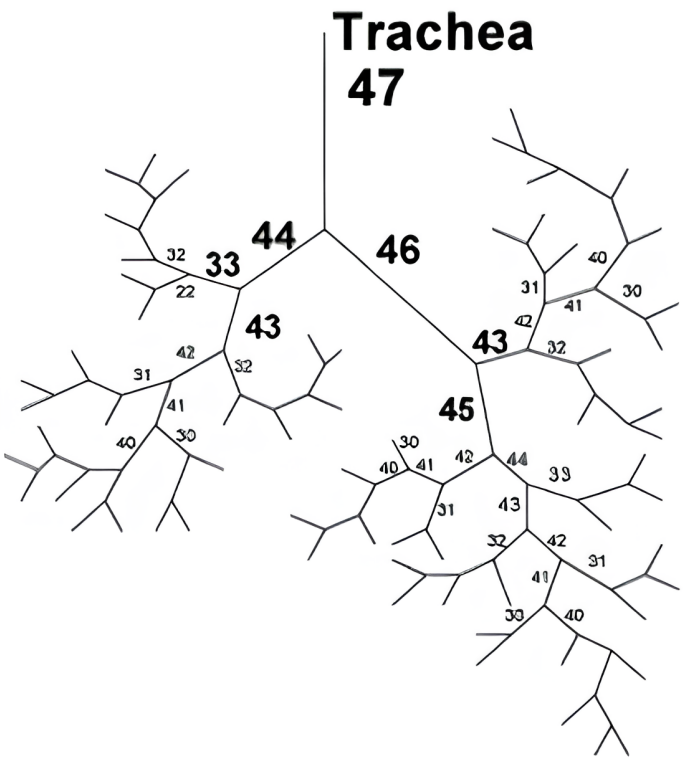

Figure 2: The dichotomous bronchial tree.

Figure 2 serves as a reference for constructing anatomically coherent adult lungs. In a dichotomous tree, each airway (excluding the trachea) has a single parent branch and two daughter branches (excluding the acini). Asymmetrical bronchial trees are a specific class presenting uneven splitting: Horsfield orders of two siblings are different (causing recursion index Δ to exist, see fig. 3). Branching angles, lengths, and diameters can vary, thus resulting in different mechanical properties.
Newborn lungs can be considered as having an analogous structure.
3D anatomical models have been generated from CTs by reconstructing the missing distal airways through algorithms[21, 19]. Model consistency was then studied, and its characteristics were compared with histological measurements[6]. Considering semilogarithmic plots of the number of branches, lengths, and diameters against Strahler orders, it is possible to define three important metrics:

R_{b}: The branching ratio. It is defined as the antilog of the *absolute value* of the slope of the number of branches. It is the factor by which the number of branches increases in successive orders *down the tree*.

R_{d}: The diameter ratio. It is defined as the antilog of the slope of the diameters. It is the factor by which the diameter increases in successive orders *up the tree*.

R_{l}: The length ratio. It is defined as the antilog of the slope of the lengths. It is the factor by which the length increases in successive orders *up the tree*.

Instead for infants, there exist models based on the ovine[8] and canine[4] anatomy.
Mathematical models developed for adult lungs cannot simply be scaled down to fit the lungs of newborns. Newborn lungs are not simply one miniature version of adult lungs, but they present significant differences in terms of bronchial branch proportions, constituents of the airways[13], morphometric characteristics (R_{d}, R_{l}, R_{b})[6] and composition[5].
Mani [12] considered an adult lung model linearly scaled to match newborn anatomical features. The advantage of this approach is that it respects the dimensions of the trachea and bronchioles. It doesn't guarantee that the morphometric characteristics of the entire airway tree are respected. In this work, a few airway generation parameters can be adapted, to better approximate the target morphometric characteristics.

4. Mechanical Model of Airways and Acini

The adult airway can be likened to a transmission line (see fig. 3), with resistors, capacitors, and inductors having constant values. These components form a circuit as illustrated. Moreover, tissues properties (Z_{w}) are incorporated. Figures 3 and 4 show modules connected according to the structure of the newborn airway, which is comparable to that depicted in fig. 2. $Z(n)$ represents the parent branch as a function of the Horsfield order, while $Z(n-1)$ and $Z(n-1-\Delta)$ denote the two daughters branches. $Z(2)$ represents the terminal airway. Each airway has a parent branch (excluding the trachea) and two daughter branches (excluding the acini).
The electrical equivalent of tissue properties is modified to test the physiological change impact on the aeration process.
The air-fluid interface modulates the values of resistances and inductances in both the module types.
Moreover, this fluid is incompressible, whereas air is not. This introduces an additional element in the electrical equivalent of air, as the compressibility of the gas is modeled through a capacitance.
During the aeration process, an air-liquid interface is created, which in turn, generates surface tension that must be overcome to allow fluid movement within the bronchial tree. Once this surface tension is overcome, the diameters can expand, leading to an increase in lung volume.
Lutchen and Gillis [9] have developed a mechanical lung model in frequency-domain, describing airways and acini modules as displayed in fig. 3 and fig. 4, respectively.

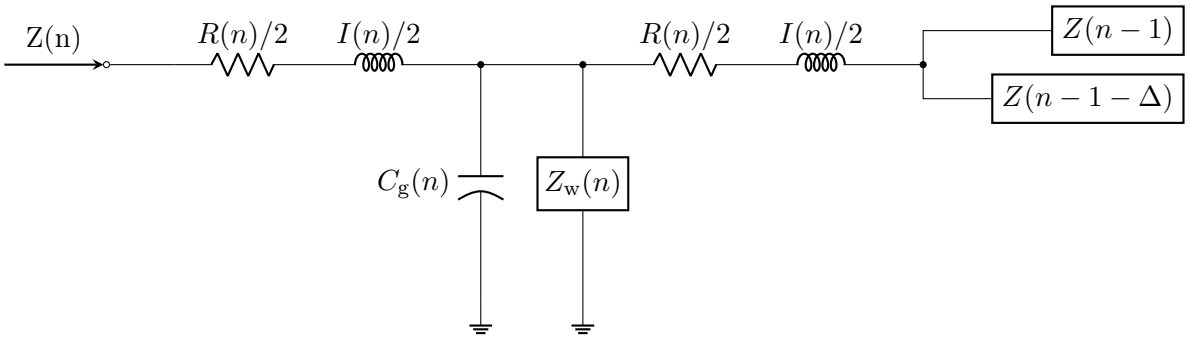

Figure 3: Impedance (Z) of a given order (n) of a single airway generation is calculated via an acoustic transmission line analysis, which accounts for shunting into gas compression in the tube ($C_{\mathrm{g}}(n)$) and into nonrigid airway walls (Z_{w}). R: resistance; Δ: recursion index[9].

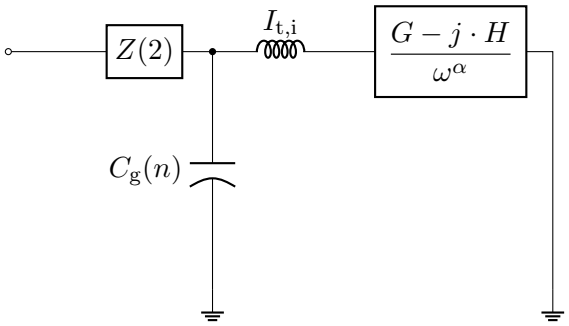

Figure 4: An alveolar-tissue element is attached to the terminal airways in the tree. There is gas compression corresponding to volume of the acinus (C_g) and the tissue element is viscoelastic containing a tissue damping (G) coupled to elastance (H) to ensure a constant tissue hysteresis. j: imaginary unit, $I_{t,i}$: tissue inertance[9].

In this thesis, as well as in [12], a mechanical model is defined in time-domain starting from the modules described in this section and properly adapted.
Capillary pressure is due to the air-fluid interface in the airway tree. It was considered and modeled as a diode component: opening threshold voltage corresponds to the aforementioned capillary pressure for a generic airway.
A first implementation has been performed on the «CADENCE» platform. This has the advantage of parallelism and speed. There are also some drawbacks to this approach: this framework is designed to simulate standard electrical components and it is not well-suited to develop time- and current integral-dependent components. Furthermore, the license is proprietary and machine-specific. This limits the accessibility of the model design process.

5. Model Development

This chapter describes the methods used to develop an open-source, 3D morphometric neonatal lung model that allows simulations of lung aeration at birth.
An anatomically coherent 3D lung model is combined with a mechanical model of the airways and acini, able to simulate changes in the mechanical properties of the airways when the lung fluid is replaced by air entering the lungs.
The sequence for model development is reported in fig. 5. We extracted a 3D surface mesh of lung lobes and airway centrelines from a lung CT of a newborn. We implemented a statistical method, previously described for adult lung models, able to generate distal airways that were not visible on the CT. We adapted the method for the newborn lung.
We implemented a mechanical model of the airways and acini whose parameters are dependent on the airway's lengths and diameters and the presence of fetal fluid, fetal fluid-air interface, or air in the airway. We exploited an open-source solver for differential equations to simulate the network.

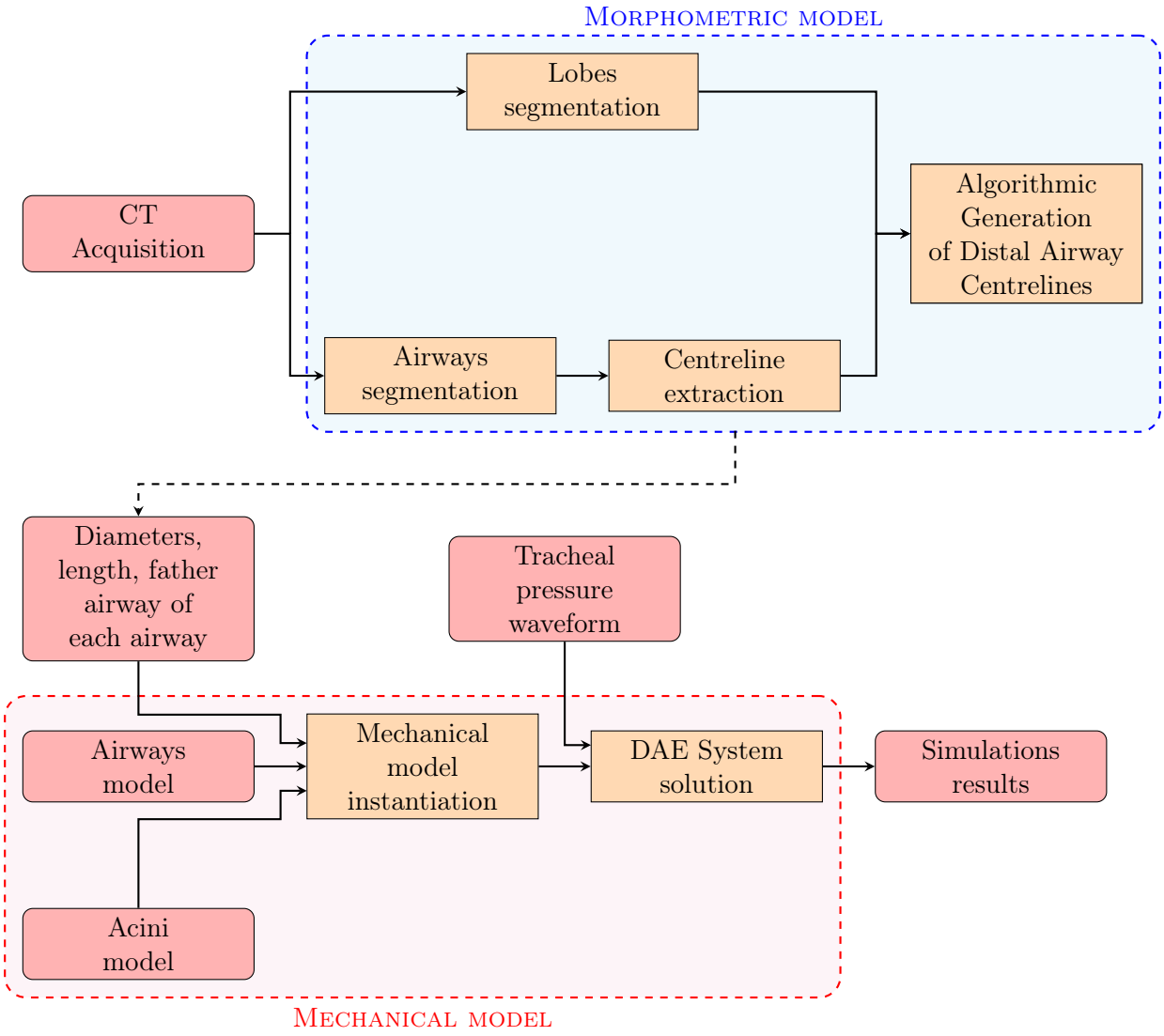

Figure 5: Data pipeline. The process begins with a *patient-specific image* (i.e. CT) of a premature newborn. The extracted data, comprising *two segmentations*, are then processed to obtain an anatomical surrogate of the airway tree. This is necessary because scanner resolution does not allow for the discrimination and localization of small branches. From the resulting morphometric model, the *mechanical parameters* can be derived, which are essential for generating an accurate simulation model. Finally, a numerical solver for differential equations provides the final output.

5.1. Anatomical Model

Morphology generation process is required as it is not possible to obtain high generations (aka small airways) using standard high-resolution CT[2].
There are different open-source platforms available for generating adult morphometric models. In particular:

1. AVATree (Windows-only)
2. Chaste (cross-platform) library

Due to problems related to «AVATree» source code compilation for Windows with «Visual Studio», Chaste library is selected for this project.
Chaste is a C++ open-source (BSD licensed) library developed by Oxford University. It has multiple use cases across various biomedical fields, with an emphasis on cardiac electrophysiology and cancer development[14]. It can be integrated into a C++ program or used via «User Project» (i.e. `ctest`). Specifically, the "AirwayGenerationTutorial" is considered as a first code base and properly adapted to match newborn parameters[20].
The required input consists of two pieces of information:

- A *mesh of centreline points*. This mesh is provided in TetGen format, comprising "airways.node" and "airways.edge" files. The first file lists centreline point coordinates, respective sampled airways radius, and a boolean value to indicate if the point is generative. The second one contains all the connections between pairs of points.
- Four (or five) *lobes segmentations* in STL format. These segmentations are necessary as they physically impose a limit on the growth algorithm.

5.1.1 CT Image Processing: Lung Segmentation, Centreline and Radii Extraction

«3D Slicer» is an open-source software used for CT image processing. Two extensions are installed:

«*Chest_ imaging_ platform*»: This extension enables semi-automatic segmentation of major airways from a single fiducial point. It can also extract adult lobes using three fiducial points per lung fissure. However, in our case, the fissures are not visible, necessitating manual intervention.

«*SlicerVMTK*»: This extension is used for extracting centreline points.

5.1.2 Algorithmic Generation of the Distal Airway Centreline

The Chaste User Project reads the input files (see section 5.1), and begins growing the anatomical surrogate from the points labeled as «generative». The algorithm operating under the hood is a modified version of the one described in [19, 2]. The generated output is available in various formats:

- VTU: Unstructured Grid (base64 encoded) format used by VTK library. It can be displayed by ParaView, an open-source viewer.
- node and edge: TetGen format. Such files are better suited for further processing.

This process is required as it is not possible to obtain high generations (aka small airways) using standard high-resolution CT[2].

The algorithm is based on a modified version of Tawhai, Pullan, and Hunter [19]. A uniform grid of seed points is created within each segmented lobar surface. Seed points approximately correspond to terminal bronchioles. The spacing of the seed point grid is set so that the mean volume around each of such points corresponds to the acinar volume (for adults being 187mm^3, for 5-weeks old newborns 5.3mm^3).

The starting points of the algorithm are the distal ends of the segmented airway centrelines. These points are referred to as growth apices.

An *adaptive threshold* on the distance between the seed points and growth apices is required to prevent spurious long airways from being generated in the last few generations. Equation (1) describes such threshold:

$$T = \max(V_\text{b} - n \cdot D_\text{l}, 5\text{mm}) \tag{1}$$

Where:

V_b is the diagonal size of the bounding box of the lobe being generated into

$D_\text{l} (= V_\text{b}/N)$ is the distance limit.

N is the maximum number of generations.

n is the current generation number.

With these definitions, the **growing algorithm** is described as such:

1. *Each seed point is associated with the closest growth apex within its lobe.* The seed point having a distance to a growth apex greater than the aforementioned adaptive threshold is not associated with that distal end. If all distal ends are further than the threshold from the seed point, the seed point remains unlabeled.
2. *Calculation of the centroid of points assigned to each distal branch.*
3. *The plane defined by the centroid and the parent branch is used to split the points into two unequal sets.*
4. *Centroids of each of the new point sets are calculated.*
5. *For each set of points a new airway is generated* starting at the distal end and extending 40% of the distance towards the centroid of the point set. This value is arbitrarily chosen for adults but kept for newborns. It must be optimized in future developments.
6. *Generated branches are checked to determine whether it is terminal.* Branches whose length is less than 2mm (for adults, to be changed with .12mm for newborns) are considered terminal. Also, branches whose point set contains just a single point are considered terminal points. For all terminal branches, their associated seed point is discarded from the global set.
7. *Iterate* until no seed point is available.

Diameters are computed by means of eq. (2).

$$\log D(x) = (x - N)\log(R_\text{d} H) + \log(D_\text{N}) \tag{2}$$

Where:

D is the airway diameter.

x is the current Horsfield order.
N is the maximum Horsfield order.
D_{N} is the maximum diameter.
$R_{\mathrm{d}}H$ is the anti-log of the slope of airway diameter plotted against Horsfield order and is set to 1.15 for adults, 1.33 for 5w newborns[6, Tab. 2]. This parameter in the code is named "DiameterRatio".

5.2. Mechanical Model

In order to perform simulation it is required to use an efficient differential equation solver. «`DifferentialEquations.jl`» wraps all available solvers (even C and FORTRAN ones) and it is very efficient [3, 17].
Julia is a free, open-source (MIT licensed), fast, scientific and numerical computing-oriented programming language. Its computational efficiency is comparable to statically typed languages like C or FORTRAN. Moreover, its high-level code expressiveness rivals that of languages like Python, R, and MATLAB[7].
Two key features, inspired by the *Lisp Language*, are highlighted here.
Metaprogramming: Code is treated as any other Julia data structure and, thus can be dynamically generated and manipulated at runtime.
Macros: They help instantiate the generated code in the body of a program.
Their importance is closely tied to the concept of Domain-Specific Languages (aka DSLs). These dialects are composed of abstractions that can be properly exploited to solve particular problems (e.g. modeling complex systems, solving differential equations).
Julia REPL has a built-in package manager (i.e. «`Pkg.jl`») used for managing project dependencies and ensuring the *repeatability* of computational setups. This is achieved by saving the required package names and commits into 'Project.toml' and 'Manifest.toml' files.

5.2.1 Programming Language — Model Designing & Instantiating

«`ModelingToolkit.jl`» encompasses all the tools necessary for model design. This Julia package is equation-driven, requiring each system to be described by Differential-Algebraic Equations (i.e. DAEs) for subsequent solving[11]. Its built-in DSL optimizes every stage of modeling, from prototyping components to instantiating the complete system.
An acausal paradigm can be adopted, allowing users to reason in terms of *components*[15]. This modularity facilitates system extensibility compared to the causal approach, where the entire system of Differential-Algebraic Equations must be considered and manually simplified[10].
In particular, the usage of `@mtkmodel` macro enables hierarchical generation of building blocks recurring in the highest-order model (i.e. «Lungs»). Here is how information is structured within `@mtkmodel` macro.

Listing 1: `@mtkmodel`: a macro for systems prototyping.

```
@mtkmodel <name_of_model> begin
    @parameters begin
        # (Optional) Some constant (e.g. Resistance, Capacitance) ...
    end
    @components begin
        # (Optional) Some dependency system (e.g. Resistor, Capacitor) ...
    end
    @variables begin
        # (Optional) Internal variables ...
    end
    @equations begin
        # Differential Algebraic Equations describing the model's behavior.
    end
    @continuous_events begin
        # (Optional) Some callback function ...
    end
end
```

Replicating the behavior of electrical components using this language is straightforward, once you are familiar with the syntax and understand the Differential-Algebraic Equations that represent their characteristics. Each generated system can then be composed into more complex ones, using the internal `@components` macro, thereby implementing the hierarchical structure mentioned earlier.

After describing the highest-order system, the Julia compiler requires its instantiation before any simulation can be performed. This is accomplished using `@mtkbuild` macro, which minimizes the number of equations that need to be solved.
Code modularity is directly reflected in the electrical equivalent circuit. Specifically, by encapsulating systems with the internal `@components` macro, it becomes possible to generate models of increasing complexity. This approach enables a clear separation between components that belong to different hierarchical levels and facilitates compartmentalization during the model design phase.

Callbacks' Role in State Variables Discontinuity Handling Not all characteristics of electrical components can be defined solely by DAEs. Voltages or currents may suddenly change, triggered by a circuit event. In such cases, *continuous callback functions* can be employed to appropriately alter the value of state variables. These callbacks consist of two functions:

- `condition`: Specifies the event to be tested.
- `affect`: Defines how the state variable(s) should be changed.

The component-based approach allows for the definition of callbacks directly within the (sub)system being modeled.

5.2.2 Airways and Acini Models

The following blocks are listed in a bottom-up order (from lowest to highest).

1. **Mathematical and Electrical Components**. The simplest blocks are derived from the standard library of components (aka «`ModelingToolkitStandardLibrary.jl`»), while integral-dependent ones rely on a modified mathematical block to manage both current integration and its timing correctly. Their behavior varies based on the neonatal pulmonary fluid interface.
   Current Integrator: it computes the current integral and manages integration timing through a Callback function (see the former Callbacks Section).
   Current Integral-Dependent Inductor: It takes the current integral value from the Current Integrator and computes the inductance value according to this formula $L(t) = L_{\text{a}} + L_{\text{b}} \cdot \left(1 - \frac{\int i(t)dt}{V_{\text{FRC}}}\right)$, where L_{a} is the inductance when air-filled, L_{b} is the difference between liquid and air inductances, V_{FRC} is the volume at FRC (i.e., Functional Residual Capacity).
   Current Integral-Dependent Resistor: It takes the current integral value from the Current Integrator and computes the resistance value according to this formula $R(t) = R_{\text{a}} + R_{\text{b}} \cdot \left(1 - \frac{\int i(t)dt}{V_{\text{FRC}}}\right)$, where R_{a} is the resistance when air-filled, R_{b} is the difference between liquid and air resistances, V_{FRC} is the volume at FRC.
   Diode: It is modeled as a voltage generator whose activation state is dependent on the fill-up states of the previous and the current module ($\text{trigger}_{\text{in}}$ and $\text{trigger}_{\text{out}}$, respectively). Its behavior is summarized by the following formula: $\Delta V = \text{trigger}_{\text{in}} \cdot (1 - \text{trigger}_{\text{out}}) \cdot V_{\text{in,th}}$, where ΔV is the voltage drop across the component and $V_{\text{in,th}}$ is the diode voltage threshold. This is a custom component and it does not come as part of the standard library.
   Inductor: Constant component.
   Resistor: Constant component.
2. **Modules**. Obtained by connecting the aforementioned components together into functional models representing a physiological structure.
   Acinus
   Airway. It has a similar behavior in comparison to a transmission line.
3. **Lungs**. They represent the highest-order model because they are a combination of acini and airways.

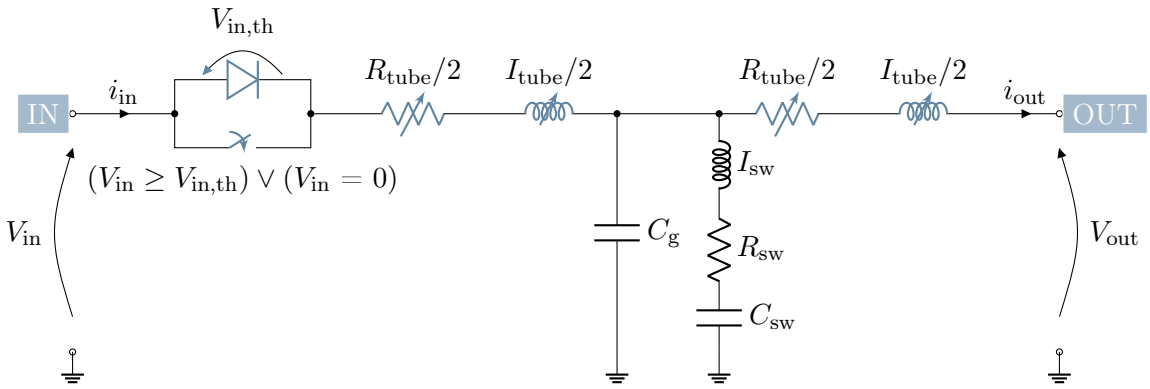

Figure 6: Airway equivalent circuit. In blue: all current integral-dependent components.

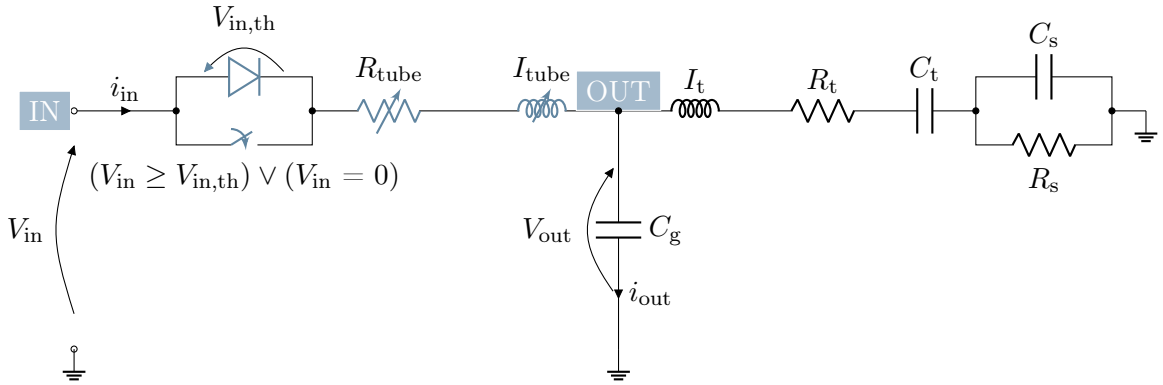

Figure 7: Acinus equivalent circuit. In blue: all current integral-dependent components.

5.2.3 Model Testing

Simulations are executed starting from a subtree (see [**fig:subtree_development**]), as the full circuit (comprising over 50k modules) requires more memory space than typically available on a common laptop.

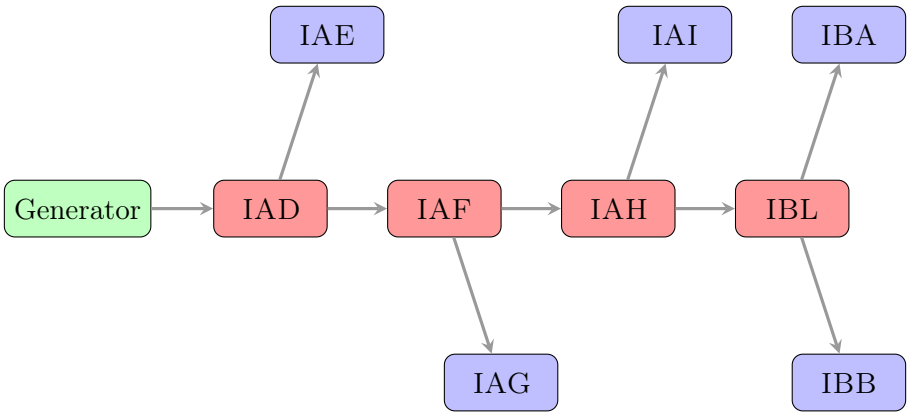

Figure 8: The simulated subtree. Airways are represented in red, acini in blue.

6. Results

6.1. Anatomical

A CT of a 40-week infant was collected. We segmented and extracted the centreline of 19 major airways, down to 5^{th} generation. We also obtained four lobes.

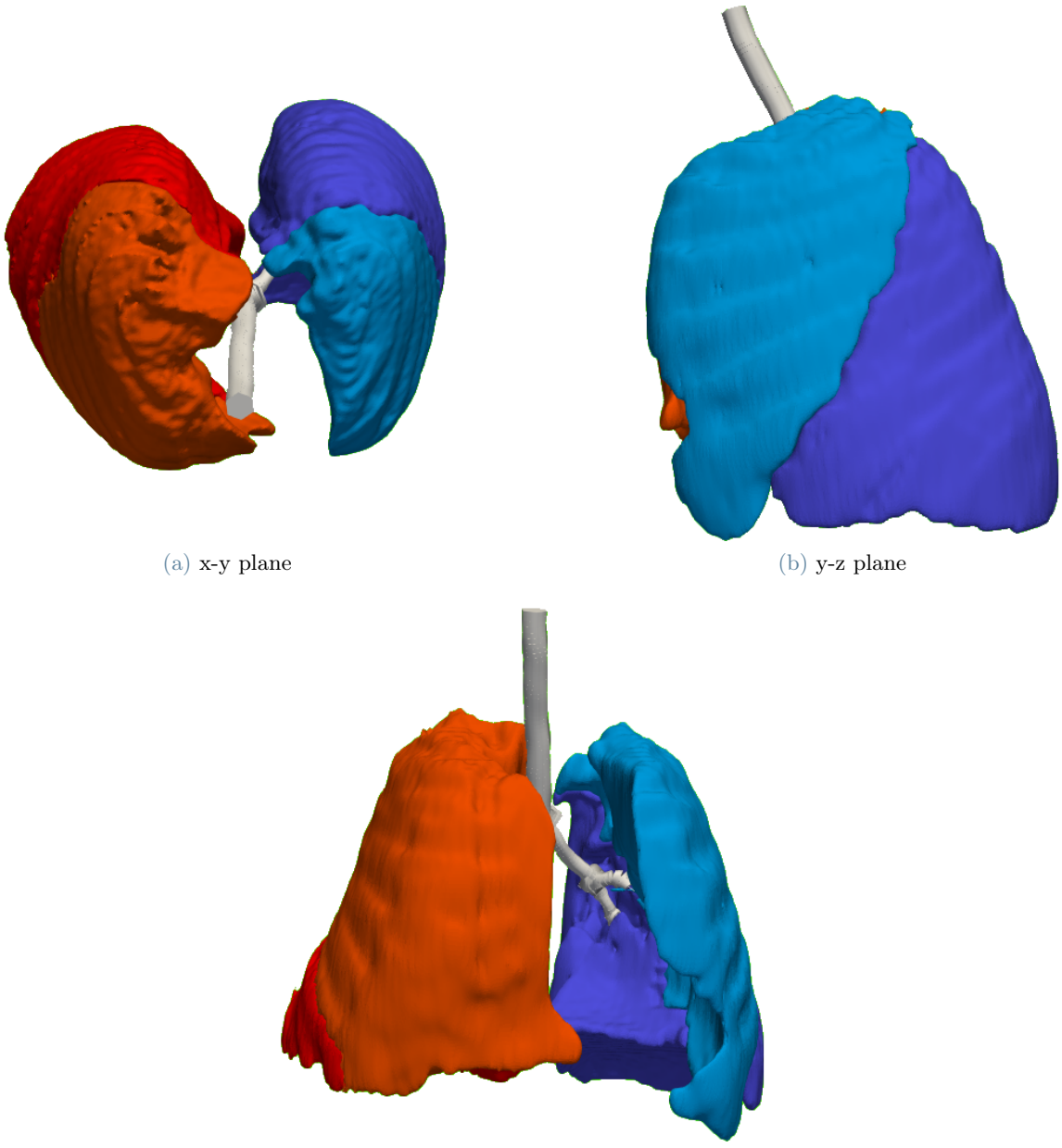

(a) x-y plane

(b) y-z plane

(c) x-z plane

Figure 9: Major Airways and Lobes segmentations. Cyan: Upper Left Lung; Blue: Lower Left Lung; Orange: Upper Right Lung; Red: Lower Right Lung.

Using the developed program, based on the Lung Chaste library, we reconstructed the missing generations starting from 15000 seed points per lung. The obtained airway tree can be displayed by ParaView.

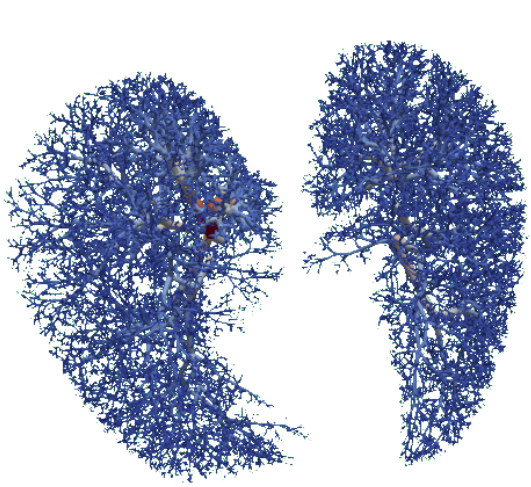

(a) x-y plane

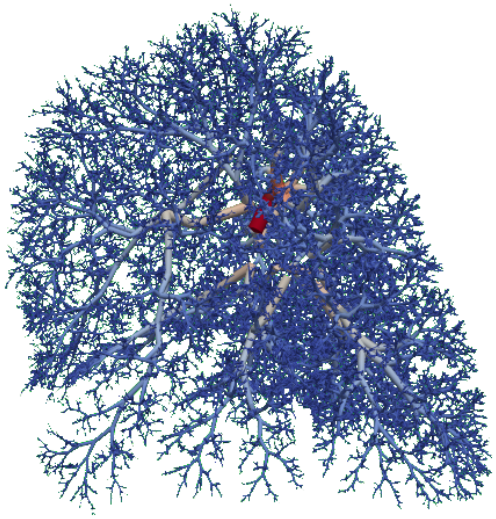

(b) y-z plane

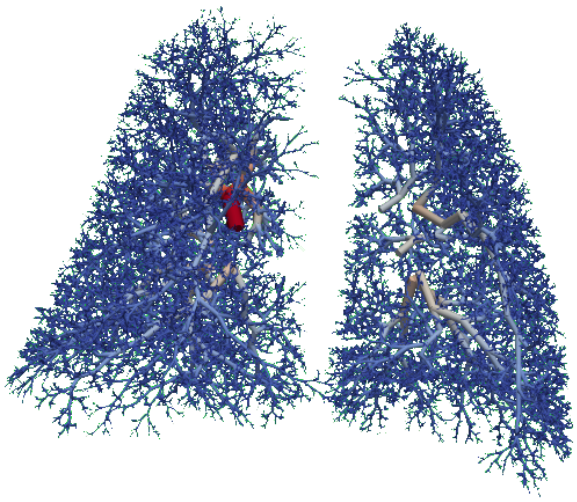

(c) x-z plane

Figure 10: Complete Airways generated by Chaste User Project (major airways are here excluded). They are color-coded with respect to their radii.

The lobes are fully covered by the statistically generated airways and this allows us to move a step forward in newborn lung simulation.

6.2. Mechanical Simulation

These simulations are to verify the various components and modules coherence. Two tests have been designed as follows. A step voltage generator is applied to the electrical equivalent of the newborn lung. The step amplitude is 10V for the first test and 8V for the second. In both tests, the step voltage is applied at $t = 1$s from the start of the simulation.
The reason why these values for voltage have been chosen is related both to the airway subtree described in Figure 8 and to the diode threshold values "vin_th" for airways and acini in Tables 1 to 4.
The first test employs a step amplitude for the voltage generator which overcomes every module diode threshold. It is possible to check out in Figures 12 and 14 modules opening times and activation orders. Airways open from the most proximal to the most distal one. It is more interesting to analyze the activation order of the acini. They open following a proximal to distal order but high diode thresholds introduce delays.

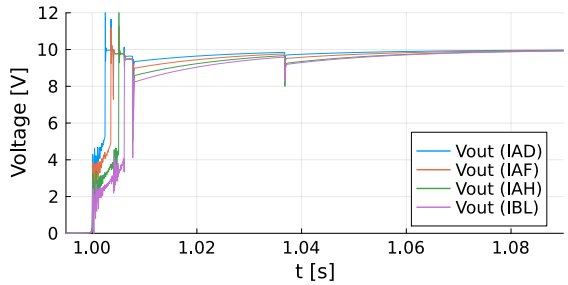

(a) Airways voltages

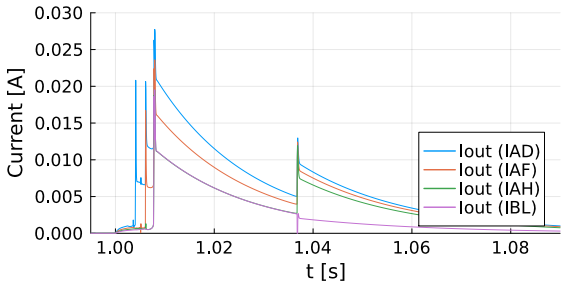

(b) Airways currents

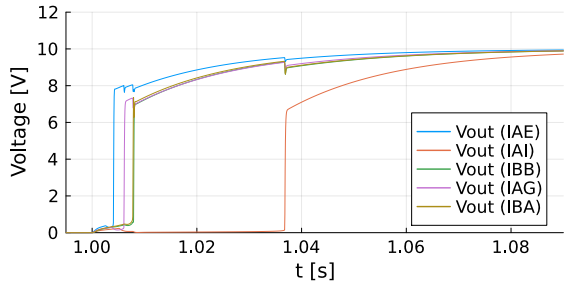

(c) Acini voltages

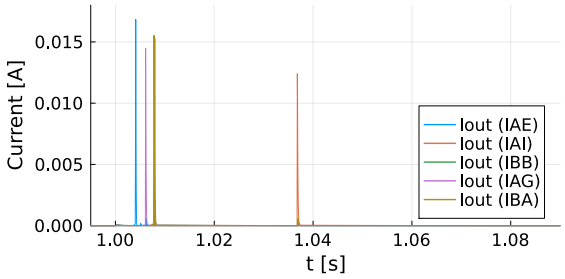

(d) Acini currents

Figure 11: (Electrically equivalent) mechanical simulation for acini and airways. The step amplitude is 10V.

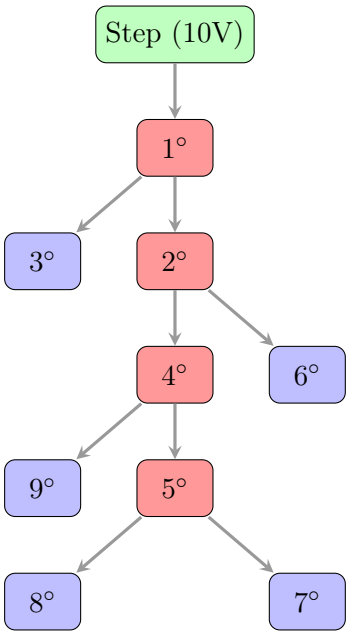

Airways	IAD	IAF	IAH	IBL
$V_{\text{in,th}}$ [V]	4.67	4.99	5.29	5.59
T_{open} [s]	1.00246	1.00356	1.00501	1.00611
Activ. order	1°	2°	4°	5°

Table 1: Airways opening times and orders when test #1 is performed.

Acini	IAE	IAG	IAI	IBA	IBB
$V_{\text{in,th}}$ [V]	7.96	8.69	9.25	6.79	7.01
T_{open} [s]	1.0041	1.0062	1.0369	1.0078	1.0080
Activ. order	3°	6°	9°	7°	8°

Table 2: Acini opening times and orders when test #1 is performed.

Figure 12: Results summary for test #1. On the left, the subtree morphology containing the opening order of each module. On the right, Tables 1 and 2 display diode thresholds and opening times.

The second test provides a voltage capable of opening some modules constituting the subtree. Opening times and activation orders are summarized into Tables 3 and 4. Relative airway activation order is increasing from proximal to distal. Only distal acini are activated due to their lower diode thresholds, the rest remain closed.

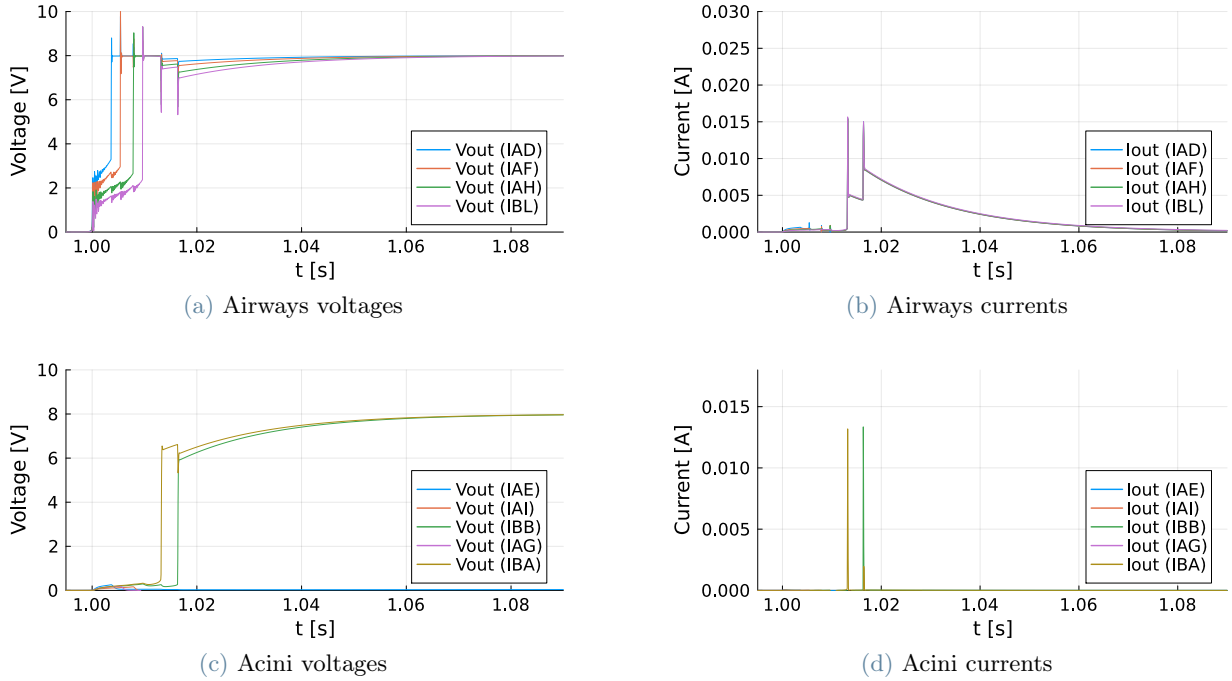

(a) Airways voltages

(b) Airways currents

(c) Acini voltages

(d) Acini currents

Figure 13: (Electrically equivalent) mechanical simulation for acini and airways. The step amplitude is 8V.

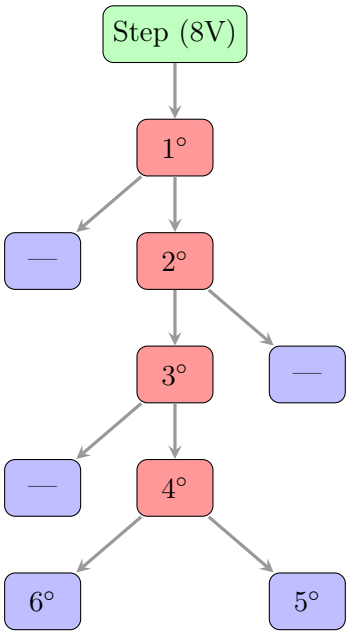

Airways	IAD	IAF	IAH	IBL
$V_{\text{in,th}}$ [V]	4.67	4.99	5.29	5.59
T_{open} [s]	1.00361	1.00536	1.00781	1.00961
Activ. order	1°	2°	3°	4°

Table 3: Airways opening times and orders when test #2 is performed.

Acini	IAE	IAG	IAI	IBA	IBB
$V_{\text{in,th}}$ [V]	7.96	8.69	9.25	6.79	7.01
T_{open} [s]	$+\infty$	$+\infty$	$+\infty$	1.01316	1.01636
Activ. order	—	—	—	5°	6°

Table 4: Acini opening times values and total activation order when test #2 is performed.

Figure 14: Results summary for test #2. On the left, the subtree morphology containing the opening order of each module. On the right, Tables 3 and 4 display diode thresholds and opening times. Long dashes: no opening has occurred.

7. Conclusion and Future Developments

Anatomical morphometric models of the adult lung have been extensively developed and used in the literature to enhance our understanding of pulmonary pathologies and to guide treatments. In contrast, anatomical morphometric models of the newborn lung are largely absent. It is not sufficient to simply scale down models developed for adult lungs to fit newborn lungs. Newborn lungs are not merely smaller versions of adult lungs; they exhibit significant differences in morphometric characteristics, airway wall structure, and tissue composition and properties. These differences must be considered when developing or adapting mathematical models to accurately represent the functioning of newborn lungs.

We developed an anatomical morphometric model of the newborn lung. Using a CT scan of a newborn infant, we extracted the centreline and the lobe surfaces. We then reconstructed the anatomy of the missing airways using a statistical algorithm originally proposed for adult lungs, which we adapted for the newborn lung. This algorithm assigned airway diameters based on proportions measured in the newborn lung, providing several advantages over previous approaches. Previous work, such as Mani [12], scaled adult models to match the diameters and lengths of the trachea and terminal bronchioles in newborns. However, this method may not accurately preserve the morphometric characteristics (R_b, R_d, and R_l – see Section 3) of the entire airway tree. Our approach allows for the direct setting of the desired R_d parameter in the model, which differs between adults and newborns. Further analysis of the generated tree can determine if all known morphometric characteristics of newborn lungs (e.g., R_b and R_l) are respected or if optimization of the arbitrary parameters initially set for adults (e.g., branching length) is necessary.

We implemented a mechanical analog of the airway and acini in Julia. This model accounts for changes related to aeration at birth, allowing the simulation of the flow of fetal fluid toward the periphery as air enters the airways. The model incorporates changes in resistance (R) and compliance (I), as well as capillary pressure developed in the airways at the fluid-air interface. Testing on a subset of the anatomical tree yielded consistent results, demonstrating the model's ability to simulate the phenomena involved in lung aeration. Future developments will include simulating the entire airway tree and analyzing the time required for full network simulation.

This model enables open-source simulation of various aeration strategies that can be applied at birth. Such simulations are crucial for defining protective lung strategies that may reduce long-term sequelae in preterm infants.

References

[1] Mary Ellen Avery, Nai-San Wang, and Jr. H. William Taeusch. *Il polmone del neonato*. 1973. URL: https://www.lescienze.it/archivio/articoli/1973/07/01/news/il_polmone_del_neonato-540585/.

[2] Rafel Bordas et al. "Development and analysis of patient-based complete conducting airways models". en. In: *PLoS One* 10.12 (Dec. 2015), e0144105. DOI: 10.1371/journal.pone.0144105.

[3] *DifferentialEquations.jl Documentation*. URL: https://docs.sciml.ai/DiffEqDocs/stable/.

[4] Jacob Herrmann, Merryn H Tawhai, and David W Kaczka. "Regional gas transport in the heterogeneous lung during oscillatory ventilation". en. In: *J. Appl. Physiol.* 121.6 (Dec. 2016), pp. 1306–1318. DOI: 10.1152/japplphysiol.00097.2016.

[5] A A Hislop and S G Haworth. "Airway size and structure in the normal fetal and infant lung and the effect of premature delivery and artificial ventilation". en. In: *Am. Rev. Respir. Dis.* 140.6 (Dec. 1989), pp. 1717–1726. DOI: 10.1164/ajrccm/140.6.1717.

[6] K Horsfield et al. "Growth of the bronchial tree in man". en. In: *Thorax* 42.5 (May 1987), pp. 383–388. DOI: 10.1136/thx.42.5.383.

[7] *Julia Documentation*. URL: https://docs.julialang.org/.

[8] Ahmed M Al-Jumaily et al. "Pressure oscillation delivery to the lung: Computer simulation of neonatal breathing parameters". en. In: *J. Biomech.* 44.15 (Oct. 2011), pp. 2649–2658. DOI: 10.1016/j.jbiomech.2011.08.012.

[9] Kenneth R Lutchen and Heather Gillis. "Relationship between heterogeneous changes in airway morphometry and lung resistance and elastance". en. In: *J. Appl. Physiol.* 83.4 (Oct. 1997), pp. 1192–1201. DOI: 10.1152/jappl.1997.83.4.1192.

[10] Yingbo Ma. *Scaling Equation-based Modeling to Large Systems*. 2024. URL: https://www.youtube.com/watch?v=c-bZ2v1uF14.

[11] Yingbo Ma et al. *ModelingToolkit: A Composable Graph Transformation System For Equation-Based Modeling*. 2021. arXiv: 2103.05244 [cs.MS].

[12] Elisa Mani. *An in-silico morphometric model of the respiratory system for simulating the dynamics of lung aeration at birth during respiratory support*. Master Thesis. June 2020. URL: https://www.politesi.polimi.it/handle/10589/165063.

[13] P J Merkus, A A ten Have-Opbroek, and P H Quanjer. "Human lung growth: a review". en. In: *Pediatr. Pulmonol.* 21.6 (June 1996), pp. 383–397. DOI: 10.1002/(sici)1099-0496(199606)21:6%3C383::aid-ppul6%3E3.0.co;2-m.

[14] Gary R. Mirams et al. "Chaste: An Open Source C++ Library for Computational Physiology and Biology". In: *PLOS Computational Biology* 9.3 (Mar. 2013), pp. 1–8. DOI: 10.1371/journal.pcbi.1002970. URL: https://doi.org/10.1371/journal.pcbi.1002970.

[15] *ModelingToolkit.jl Documentation*. URL: https://docs.sciml.ai/ModelingToolkit/stable/.

[16] The World Health Organization. *Preterm birth*. 2013. URL: https://www.who.int/news-room/fact-sheets/detail/preterm-birth.

[17] Chris Rackauckas, Christopher, and Qing Nie. "DifferentialEquations.jl–a performant and feature-rich ecosystem for solving differential equations in Julia". In: *Journal of Open Research Software* 5.1 (2017). DOI: 10.5334/jors.151.

[18] Béla Suki, Dimitrije Stamenović, and Rolf Hubmayr. "Lung parenchymal mechanics". en. In: *Compr. Physiol.* 1.3 (July 2011), pp. 1317–1351. DOI: 10.1002/cphy.c100033.

[19] M. Howatson Tawhai, A. J. Pullan, and P. J. Hunter. "Generation of an Anatomically Based Three-Dimensional Model of the Conducting Airways". In: *Annals of Biomedical Engineering* 28.7 (July 2000), pp. 793–802. ISSN: 1573-9686. DOI: 10.1114/1.1289457. URL: https://doi.org/10.1114/1.1289457.

[20] *TestAirwayGeneration (Chaste Tutorial)*. URL: https://chaste.github.io/docs/user-tutorials/airwaygeneration/.

[21] Nora T Tgavalekos et al. "Relation between structure, function, and imaging in a three-dimensional model of the lung". en. In: *Ann. Biomed. Eng.* 31.4 (Apr. 2003), pp. 363–373. DOI: 10.1114/1.1557972.

Sommario

Durante la gravidanza, le vie aeree fetali sono riempite con un liquido noto come fluido polmonare fetale, essenziale per lo sviluppo delle vie aeree. Di conseguenza, alla nascita, il sistema respiratorio deve espellere questo liquido per permettere l'aerazione. I neonati pretermine potrebbero non essere in grado di raggiungere in modo autonomo l'aerazione polmonare alla nascita. L'applicazione di una forma d'onda di pressione positiva all'apertura delle vie aeree può supportarli. Tuttavia, la migliore strategia di pressione per promuovere l'aerazione polmonare senza danneggiare il fragile polmone è ancora sconosciuta. La simulazione del modello può aiutare nella definizione di tale strategia. Gli obiettivi di questo progetto sono: 1) Generare un modello a partire dalle scansioni TC neonatali per ottimizzare la generazione delle vie aeree, assicurando che aderiscano alle caratteristiche morfometriche a diverse età. 2) Sviluppare un modello meccanico open-source che consenta la simulazione delle proprietà meccaniche insieme alla dinamica dei fluidi. Utilizzando una scansione TC di un neonato, abbiamo estratto la linea centrale delle principali vie aeree e le superfici dei lobi. Successivamente, abbiamo ricostruito l'anatomia delle vie aeree mancanti utilizzando un algoritmo statistico originariamente proposto per i polmoni degli adulti, che abbiamo adattato per il polmone del neonato. Questo algoritmo ha assegnato i diametri delle vie aeree in base alle proporzioni misurate nel polmone del neonato. Abbiamo implementato un analogo meccanico delle vie aeree e degli acini in Julia. Questo modello tiene conto dei cambiamenti relativi all'aerazione alla nascita, permettendo la simulazione del flusso del liquido fetale verso la periferia mentre l'aria entra nelle vie aeree.

Parole chiave: modello morfometrico, processo di aerazione, polmone, neonato, sistema respiratorio